USE OF A CONVOLUTION METHOD AT LINEAR INTERVALS IN X-RAY DIFFRACTION PROFILES

EMPLEO DE MÉTODO DE CONVOLUCIÓN A INTERVALOS LINEALES EN PERFILES DE DIFRACCIÓN DE RAYOS-X

D. M. Rodríguez-Herrera[a], A. Pentón-Madrigal[b†], E. Estevez-Rams[b]

a) Department of Physics and Engineering Physics, University of Saskatchewan, Saskatoon SK S7N 5E2, Canada.
b) Facultad de Física - IMRE, Universidad de La Habana, Cuba. arbelio@fisica.uh.cu.†
† corresponding author

Recibido 20/02/2024; Aceptado 28/03/2024

Se presenta un formalismo matemático para el cálculo del perfil intrínseco de un máximo de difracción a través de un proceso de convolución usando un conjunto de funciones lineales por intervalos. Este proceso de convolución es implementado en el formalismo para la solución directa de un patrón de difracción de una estructura cristalina de capas afectada por defectos planares. Este procedimiento permite calcular la longitud de correlación (Δ_C), cantidad que describe el grado de desorden en este tipo de estructuras cristalinas. El resultado obtenido es validado a través del método de Warren – Averbach para el análisis microestructural.

A mathematical formalism for calculating the intrinsic profile of a diffraction maximum through a convolution process using a set of linear functions by intervals is presented. This convolution process is implemented in the formalism for the direct solution of a diffraction pattern of a layered crystalline structure affected by planar defects. It allows the correlation length (Δ_C) to be calculated, which describes the degree of disorder in this type of crystalline structure. The obtained result is validated through the Warren–Averbach method for microstructural analysis.

PACS: X-ray diffraction (difraccón de rayos-X), 61.05.cp; microestructure (microestructura), 61.72.-y; Crystal defects (defectos cristalinos), 61.72.-y; Fourier analysis (Análisis de Fourier), 02.30.Nw.

I. INTRODUCTION

The physical and chemical properties of polycrystalline solids depend directly on their structure and microstructure. Their detailed study is decisive for the understanding and design of those properties. The microstructure of a solid includes the size and distribution of crystallites (coherent domains), grain sizes and their orientation, the interaction between their boundaries, the density and types of crystalline defects causing of the crystalline structure, its chemical composition and the number of the existing phases [1,2].

The central point of materials science is to develop models and methods that, together with appropriate characterization techniques, allow the establishment of the relationship between microstructure and properties. X-ray diffraction (XRD) is a non-destructive and essential technique to obtain information on the structure and microstructure of materials.

Microstructural analysis methods by XRD are necessarily linked to the fitting of diffraction maxima. In the experimental data, these maxima appear as a convolution of functions, since the instrument's contribution and the sample's microstructure are contained in the observed profile [3]. The separation of both contributions is known as line profile analysis [4–6], and constitutes one of the practical aspects of experimental X-ray data reduction prior to a microstructural analysis.

The experimentally observed diffraction maximum profiles f(θ) result from the convolution of two functions: the instrumental contribution g(θ) and the sample's contribution (intrinsic profile) h(θ) [7,8]. The convolution is defined as:

$$f(\theta) = g(\theta) \otimes h(\theta) = \int_{-\infty}^{+\infty} h(\tau) g(\theta - \tau) d\tau \tag{1}$$

The function g(θ) can be determined in two ways: (i) by using the "fundamental parameter approach" method [9] or (ii) by measuring the diffraction pattern of a standard sample. Once the functions f(θ) and g(θ) are determined, then h(θ) can be obtained.

II. CONVOLUTION PROCESS

The classical Stokes method [6] for numerical convolution of equation (1) is not appropriate due to the oscillations introduced in h(θ) as a result of the method's sensitivity to statistical errors in experimental data [10].

The convolution of analytical functions for modeling the instrumental contribution has been used as an alternative method [11] but the operation may consume significant computing time. A solution to this problem is presented in [9] where the integral in equation (1) is reduced to a sum over appropriate intervals. It is assumed that within each of these intervals, the function to be convolved is a polynomial connecting adjacent points, resulting in a continuous function.

The use of series expansions for the convolution of diffraction profiles has also been discussed by Sanchez-Bajo, F. &

Cumbrera, F. L. [12] and implemented in the direct solution of a diffraction pattern of a layered crystal structure affected by planar defects [13].

It is known that pure Gaussian and Lorentzian functions do not appropriately describe diffraction profiles [14]. Instead, analytical functions such as the Voigt function [15], the pseudo-Voigt function [16, 17], and the Pearson-VII function [18] are used, which are more flexible in accommodating a variety of possible profiles. Using Voigt functions is appropriate for instrumental broadening [19] but their analytical expression is more complex than the pseudo-Voigt (pV) function. The pV function is defined as a linear combination of a Gaussian function and a Lorentzian function.

To circumvent the above mentioned complexity, a method is implemented in this work that provides a solution to Equation (1), and generalizes the convolution process of the formalism presented in [13]. The proposed formalism is built on the concept introduced by [9], where the integral (1) is converted into a summation of functions. As an example of application, the diffraction maxima of crystals affected by planar defects are used.

To numerically solve Equation (1), the normalized function h(θ) is described by a pV function with adjustable parameters. To remove the instrumental component g(θ), it is represented as a set of piecewise linear functions, meaning small intervals of the original function are taken and fit with straight segments:

$$g(\theta) = y_1(\theta) + y_2(\theta) + ... + y_n(\theta) \tag{2}$$

such that:

$$y_n(\theta) = (m_n\theta + n_n)H(\theta - \theta_{min_n})H(\theta_{max_n} - \theta)$$

varies smoothly and continuously, and where $m_n\theta + n_n$ are linear functions of slope m_n and intercept n_n. H represents the heaviside unit step function [20], θ_{min_n} and θ_{max_n} are the minimun and maximun values of θ within each interval respectively, where $\theta_{max} - \theta_{min}$ is the length of each interval.

The chosen interval is equivalent to the 2θ step of the experimental data, which does not exceed 5 % of the value of the full width at half maximum (FWHM). These functions, being linear, can be convolved within each interval with the function h(θ). Equation (1) then results in:

$$c_n(\theta) = y_n(\theta) \otimes h(\theta) \tag{3}$$

and a set of functions $c_n(\theta)$ representing each interval of the original function is obtained after the convolution process. These functions contain the adjustable parameters of a pseudo-Voigt function, that is, they contain the adjustable parameters of h(θ). Due to the linearity properties of the convolution, one gets:

$$f(\theta) = \sum_{i}^{n} c_i(\theta) \tag{4}$$

The fitting of f(θ) according to (4) yields the values of the parameters of the pV function h(θ), which contains information about the microstructure of the sample under study. The numerical solution process described for the equation (1) is depicted in Fig. 1.

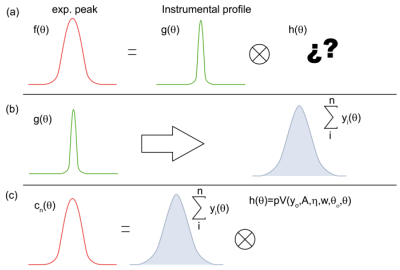

Figure 1. Convolution process in three parts: (a) Problem formulation, (b) Segmentation of the instrumental function, (c) Convolution of the sum of linear functions with a pseudo-Voigt function for fitting the f(θ) data.

Even though the maxima generated by numerical convolution processes should be normalized, the use of multiple linear functions in the calculation breaks this normalization. As a result, the maximum must be renormalized in the final phase of the process.

III. VALIDATION OF THE CONVOLUTION PROCESS

The convolution process is validated in the mathematical formalism for the direct solution of the diffraction pattern of a layered crystal with stacking faults [13, 21, 22], and the results are compared with the standard Warren-Averbach method [23, 24].

III.1. Method: Direct solution (DS) of the diffraction pattern of a layered crystal with planar defects

This formalism is discussed in detail in [13,21,22] and outlined here. It allows for determining the degree of disorder in a stacking sequence of a layered crystalline structure due to the occurrence of planar defects. A Fourier series can represent the diffraction pattern of a layered crystalline structure:

$$\vec{r}^* = 1 + 2\sum_{\Delta=1}^{\infty} A_\Delta cos(2\pi\Delta l) + B_\Delta sin(2\pi\Delta l) \tag{5}$$

where is the interference function proportional to the diffracted intensity by the crystal and it is defined in reciprocal space. The coordinate takes continuous values in the direction of the reciprocal axis c^* and Δ is the number of layers perpendicular to the stacking direction in the crystal. The

Fourier coefficients can be directly determined from the diffraction pattern as follows:

$$A_\Delta = \int_{-\frac{1}{2}}^{\frac{1}{2}} Q(\vec{r}^*)cos(2\pi\Delta l)dl \qquad \Delta = 1, 2, ... \tag{6}$$

In a polycrystal with random orientation, the coefficients $B_\Delta = 0$, while the coefficients A_Δ can be expressed as a sum of integrals over each diffraction maximum within the integration range [22]:

$$A_\Delta = cos(2\pi\Delta l_{oi}) \int_{-(\frac{1}{2}+l_{oi})}^{\frac{1}{2}-l_{oi}} v_i(l)cos(2\pi\Delta l)dl$$
$$-sen(2\pi\Delta l_{oi}) \int_{-(\frac{1}{2}+l_{oi})}^{\frac{1}{2}-l_{oi}} v_i(l)sin(2\pi\Delta l)dl \,, \tag{7}$$

where the function $v_i(l)$ denotes the i-th maximum within the integration range. The first term being the symmetric part of $v_i(l)$; the second term describes the asymmetric component. The terms outside the integrals determine the periodic oscillatory behavior in A_Δ.

Conversely, the integrals result in a Dirac delta function for a perfectly periodic stacking. In the case of a crystal with planar defects, the integral describes a profile of a maximum with broadening. In this case, the term within the integral will give a damped oscillatory function that tends to zero with the increase of Δ [22].

The damping term, which depends on the shape and width of the peak, will be the sole element determining the value of the correlation length Δ_c (expressed in number of layers) in the stacking sequence. This magnitude takes into account the loss of correlation between atomic layers in the stacking with the increase of Δ due to the occurrence of planar defects in the structure [13]. Considering equation (7) as valid, the following analytical function can be proposed for fitting the diffraction maxima affected by planar defects [25, 26]:

$$v_\Delta(l) = v_o CG^C_\Delta(l) + SG^S_\Delta(l) \,, \tag{8}$$

where $v_\Delta(l)$ is the diffraction peak profile in reciprocal space, which has been subjected to the reduction process of experimental data (h(θ)). In equation (8), $CG^C_\Delta(l)$ and $SG^S_\Delta(l)$ are the symmetric and asymmetric components of the pV function used in this study:

$$G^C_\Delta = \frac{1}{2}\sum_{\Delta=1}^{\infty} exp(-f(\Delta))cos(2\pi\Delta(l_o - l)) \tag{9}$$

$$G^C_\Delta = \frac{1}{2}\sum_{\Delta=1}^{\infty} exp(-f(\Delta))sin(2\pi\Delta(l_o - l)) \,, \tag{10}$$

where $f(\Delta)$ is a positive, non-decreasing function of Δ.

III.2. The pseudo-Voigt function

The pseudo-Voigt function (pV) is expressed as a linear combination of Gaussian and Lorentzian functions:

$$pV * (\vec{r}^*) = \eta G(\vec{r}^*) + 1(1-\eta)L(\vec{r}^*) \,, \tag{11}$$

where η is a weight coefficient of both components.

The exponential decay term $exp(-f(\Delta))$ for the pV function is obtained by solving the integrals in equation (7), resulting in the final expression for equation (8) as:

$$v_\Delta(l) = \sum_{\Delta=1}^{\infty} \eta exp[(-\frac{\Delta}{\Delta_c})^2] + (1-\eta)exp[-\frac{\Delta}{\Delta_c}]$$
$$(cos[2\pi\Delta(l_o - l)] + sin[2\pi\Delta(l_o - l)]) \tag{12}$$

The function $v_\Delta(l)$ representsthe function h(θ) in the reciprocal space.

III.3. The Warren –Averbach (WA) method

The WA method [23, 24] is employed in "single peak"mode analysis, whereby it is considered, a priori, that the only contribution to the diffraction peak width results from the average coherent domain size $\langle D\rangle^{(hkl)}_{WA}$. This magnitude can be compared with Δ_c if one takes into account the layer spacing along the same crystallographic direction. In this particular case, both methods can be applied to assess the occurrence of planar defects in layered crystal structures.

The WA method is also based in equation (5) and in this case the Fourier coefficients would be determined solely by the contributions of the $A^\Delta_{\langle D\rangle}(L)$ coefficients, which represent the contributions of $\langle D\rangle^{(hkl)}_{WA}$

$$A_\Delta(L) = A^{\langle D\rangle}_\Delta(L) \,, \tag{13}$$

where L is the crystal column lengthperpendicular to the lattice plane in Bragg condition. Once a specific analytical function is chosen to fit a peak, the A_Δ coefficients can be directly calculated. Once the coefficients are determined, they are used to calculate the magnitudes of interest ($\langle D\rangle^{WA}_{(hkl)}$) by applying the procedure established in this method, which has been widely disseminated in the literature [23, 24].

Finally, it should be remarked that in both presented methods (DS and WA), the "single peak" analisys will be implemented, using only those diffraction maxima affected by planar defects.

IV. EXPERIMENTAL RESULTS

IV.1. Layered crystal structure affected by planar defects

The Al_xTi_{3-x}, x = 0.20(AlTi_20) alloy crystallizes in a hexagonal layer structure (hcp) with space group $P6_3/mmc$ (ICSD #43416) [27].

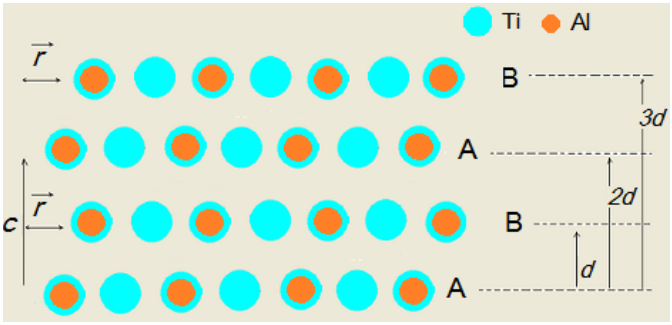

Figure 2. Visualization of the stacking of atomic layers along the [001] direction.

Figure 2 shows the projection, along the [001] crystallographic direction, of the atomic layers stacking separated at a distance d. Each layer within the unit cell is represented by the A and B letters. Both atomic layers are similar, but displaced laterally with respect to each other by a fraction of a lattice translation vector: $s\vec{r} = s(\frac{\vec{a}}{3} + \frac{\vec{b}}{3})$ with $s = 0(A), 1(B) \wedge 2(C)$.

The vectors $\vec{a}$ and $\vec{b}$ define the basal plane of the unit cell.

In the presence of a perfect hexagonal structure, the stacking sequence of the atomic layers would be represented by: ...ABABAB... along [001].The interlayer distance (d) depends on the alloy composition.

In real crystals, planar defects collapse the perfect hexagonal stacking sequence when atomic layers of the $s = 2(C)$ type are introduced. Any variation in the perfect stacking sequence will be reflected in the width and asymmetry of certain X-ray diffraction maxima.

IV.2. Diffraction pattern affected by planar defects

The XRD pattern of the AlTi_20 powder sample was recorded at room temperature in a Pert Panalyticaldiffractometer in Bragg – Brentano configuration, angular range: $2\theta = 15° - 90°$, with $\Delta 2\theta = 0.02°$. The radiation used was $C_{k\alpha 1,k\alpha 2}$ operating the equipment at 35 kV and 20 mA. The sample was mounted on a rotating sample holder to improve statistics in the number of counts. A LaB6standard sample was measured under the same conditions to take into account instrument contributions to the diffraction maxima width and to correct for instrumental zero in the determination of the alloy´s unit lattice parameters.

Figure 3 shows the (101) and (202) reflections of the normalized experimental diffraction pattern. These reflections have been selected for analysis because they satisfy:

$$h - k \neq= 3n\ ,n \in \not\in \qquad (14)$$

which establishes the condition of being affected by planar defects [13,21,22].

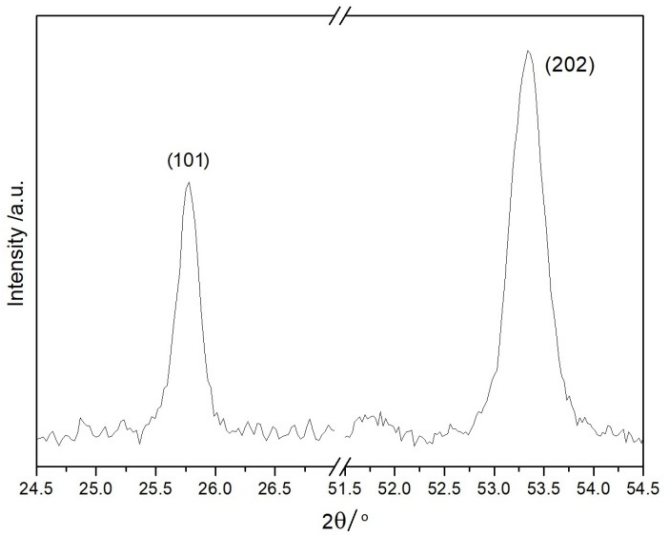

Figure 3. (101) and (202) diffraction maxima of the AlTi_20 alloy.

IV.3. Convolution

Once the $Cu_{k\alpha 2}$ component has been removed using a modification of well-established formalisms [28, 29] and subtracting the background contribution from the diffraction maximum, the convolution process described in session 2 is performed. It must be remembered that the functions $g(2\theta)_{(hkl)}$ represent the diffraction maxima of the standard sample angularly close to the reflections $g(2\theta)_{(hkl)}$ of the AlTi_20 sample.

According to equation (5), the deconvolved profiles $h(2\theta)_{(101)}$, $h(2\theta)_{(202)}$ (solid curves) are obtained from the observed $f(2\theta)_{(101)}$, $f(2\theta)_{(202)}$ maxima (dotted curves) (Fig. 4).

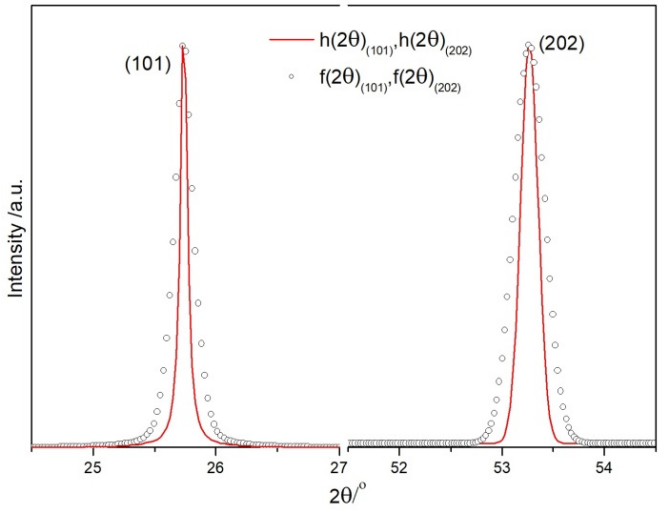

Figure 4. Observed diffraction maxima $f(2\theta)_{(101)}$, $f(2\theta)_{(202)}$ (dotted curves) and deconvolved profiles $h(2\theta)_{(101)}$, $h(2\theta)_{(202)}$ (solid curves).

IV.4. Determination of Δ_C and $\langle D\rangle^{WA}_{(hkl)}$

The $h(2\theta)_{(101)}$, $h(2\theta)_{(202)}$ maxima are transformed from the 2θ space to l space, a coordinate that takes continuous values in the direction of the reciprocal c* axis. For the space transformation, the unit cell parameters determined by a standard least squares method were used. Fitting the functions $h(l)_{(101)}$, $h(l)_{(202)}$ by least squares (Fig. 5) using equation (11) results in the parameters reported in table 1.

It should be noted that as a result of the convolution process, a narrower profile than the original is obtained, which will necessarily lead to a reduction of the points describing the intrinsic profile of the sample (Fig. 5). To maintain an appropriate number of points describing the deconvolved peak profile, the experimental peak should be measured with a smaller step ($\Delta 2\theta$). However, the fit obtained from both profiles still constitutes an acceptable result to determine the parameters reported in table 1.

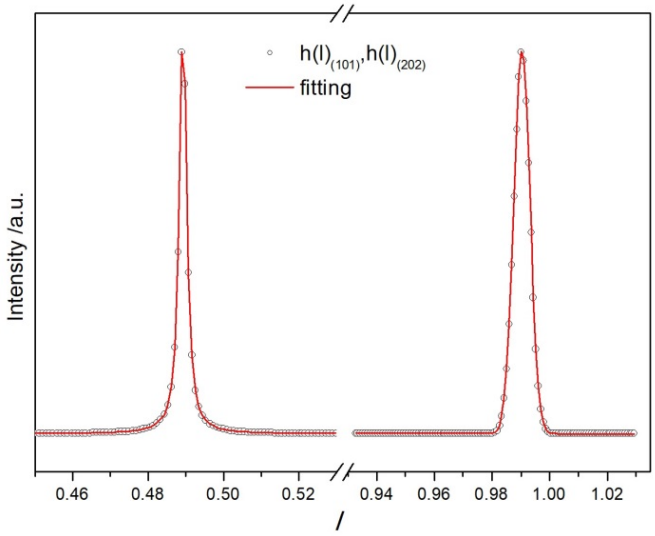

Figure 5. Fitting (solid curve) of the functions $h(l)_{(101)}$, $h(l)_{(202)}$ (dotted curve) with equation (11).

Table 1. Fitted parameters values of $h(l)_{(hol)}$ and coherent domain length.

Parameters	(101)	(202)
l_o	$0.489 \pm 2{\cdot}10^{-3}$	$0.990 \pm 2{\cdot}10^{-3}$
Δ_C / No. of layers	143 ± 10	80 ± 10
$(\Delta_C\text{-}1)\frac{c}{2}$ (nm)	33 ± 2	18 ± 2

The magnitude $(\Delta_C - 1)c/2$, where $c/2$ is the interlayer spacing along the crystallographic direction and c = 0.466(9) nm (the lattice parameter) allowexpressing the correlation length (Δ_C) in terms of a coherent domain length along the direction [001].

The Warren-Averbach method was applied to the same reflections under the considerations made in section III.3, using the WinFit software [30]. Figure 6 shows the dependence of the Fourier coefficients on L for both reflections. From the intercept with the abscissa axis of the tangent to the curve in $L \to 0$, the average values of the coherent domain are obtained: $\langle D\rangle^{WA}_{(101)}$ = (40 ± 1) nm for the (101) reflection and $\langle D\rangle^{WA}_{(202)}$ = (21 ± 1) nm for the (202).

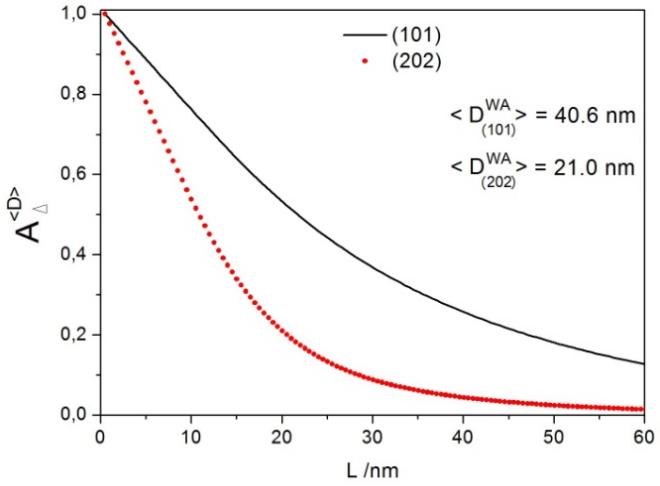

Figure 6. Fourier coefficients of (101) and (202) as function of L.

To compare the coherent domain values obtained **through** both methods, it is necessary to take into account the projection of the quantities $\langle D\rangle^{(hkl)}_{WA}$ along the [001] direction. Once the angle between the lattice planes (101) and (001) in the hexagonal system has been determined, the values of the projections are: $\langle D\rangle^{WA}_{(101)}$ = (29 ± 1) nm and $\langle D\rangle^{WA}_{(202)}$ = (15 ± 1) nm .

These values can be considered similar to those reported in Table I. This result allows to generalize the convolution process in the formalism *"direct solution of the diffraction of a layer crystal with planar defects"* [13, 21, 22].

The difference in the calculated values for the coherence length from both reflections results from not having considered in either of the two methods the contributions of non-uniform microstrains to the width of the diffraction maxima, a contribution that increases with the increase of the (hkl) indices values.

Another aspect to consider is that the calculated values of coherence length do not distinguish between the contributions due to crystallite size and contributions from stacking faults; in fact, both contributions are classified as of "effective size effect" type [23]. Well-established procedures exist in the literature to separate these contributions [31], where reflections that meet and do not meet the condition given by (13) are employed. The mentioned limitations do not affect the fundamental purpose of this article, which is the validation of the formalism presented in section II.

The use of the DS method also provides information about the position of a peak in l space, while the WA method does not. For an ideal hex.sequence, the positions of (101) and (202) reflections should be at l_o = 0.5, l_o = 1 respectively. The shift of the peaks with respect to their ideal position, although not significant in this case, usually provides information about an emerging change in the stacking period due to the occurrence

of planar defects.

V. CONCLUSION

A new convolution method for calculating the intrinsic profile of a diffraction maximum was used during the experimental data reduction process of a diffraction pattern for a specific system. The calculation of the coherence length from the correlation length within the framework of the DS method using a pV function with an exponential decay term proved to be robust. The calculated values coincide with those calculated from the WA method. The described convolution procedure has been implemented in Wolfram Mathematica [32] and is available upon request to the authors.

VI. ACKNOWLEDGMENTS

This work was supported in the framework of a scientific project associated to the national program of fundamental science (MES–UH-2018). Dr. A. Fundora is also acknowledged for providing the X-ray diffraction facility. The authors thank Aleida Pentón for editing the figures.

REFERENCES

[1] Robert L. Snyder, JaroslavFiala and Hans J. Bunge, "Defects and Microstructure: Analysis by Diffraction", (Edit. IUCr Oxford Science Publications, 2000).

[2] E.J. Mittemaijer, and P. Scardi, "Diffraction Analysis of the Microstructure of Materials", (Springer, Berlin, 2004).

[3] R.L. Snyder, "The Rietveld Method", (Oxford University Press, 1993).

[4] A.J.C. Wilson, "X-Ray Optics", (Methuen, London, 1962).

[5] A. V. Rozhkov, A. O. Sboychakov, A. L. Rakhmanov, and F. Nori, Phys. Rep. **648**, 1 (2016).

[6] A. R. Stokes, Proc. Phys. Soc. **61**, 382 (1948).

[7] A. J. C. Wilson, "Mathematical Theory of X-ray Powder Diffractometry", (New York: Gordon & Breach, 1963).

[8] H. P Klug, & L. E. Aiexander, "X-ray Diffraction Procedures", (New York: Wiley-Interscience, 1974).

[9] R. W. Cheary, and A. Coelho, J. Appl. Cryst. **25**, 109 (1992).

[10] R. Croche, and L. Gatineau, J. Appl. Cryst. **10**, 479 (1977).

[11] S. Enzo, G. Fagherazzi,A. Benedetti, and S. Polizzi, J. Appl. Cryst. **21**, 536 (1988).

[12] F. Sánchez-Bajo, and F. L. Cumbrera, J. Appl. Cryst. **33**, 259 (2000).

[13] E. Estevez-Rams, A. Penton-Madrigal, R. Lora-Serrano, J. Martínez-García, J.Appl. Cryst. **34**, 730 (2001).

[14] H. C. Van De Hulst, and J. J. M. Reesinck, Astrophys J. **106**, 121 (1947).

[15] H. T. De Keijser, J. I. Langford, E. J. Mottemeijer, and A. B. P. Vogels, J. Appl. Cryst. **15**, 308 (1982).

[16] G. K. Wertheim, M. A. Butler, K. W. West and D.N.E. Buchanan, Rev. Sci. lnstrum. **11**, 1369 (1974).

[17] P. Thompson, D. E. Cox, J. B. J. Hastings, Appl. Crystallogr. **20**, 79 (1987).

[18] T. Ida, M. Ando, and H. Toraya , J. Appl. Cryst. **33**, 1311 (2000).

[19] J. I. Langford, .Accuracy in Powder Diffraction", (US Dept. of Commerce, Gaithersberg, 1980).

[20] J. M. Marín Antuña, "Teoría de funciones de variable compleja", (Primera edición, Editorial Universitaria, 2014).

[21] E. Estevez-Rams, J. Martinez, A. Penton-Madrigal, R. Lora-Serrano, Phys. Rev. B **63**, 54109 (2001).

[22] E. Estevez-Rams, B. Aragon-Fernández, H. Fuess, and A. Penton-Madrigal. Phys. Rev. B **68**, 064111 (2003).

[23] B.E. Warren, "X-ray diffraction", (Addison-Wesley, 1969).

[24] B.E. Warren, ActaCryst. **8**, 483 (1955)

[25] E. Estevez-Rams, M. Leoni, B. Aragon-Fernández, P. Scardi, and H. Fuess, Philosophical Magazine **83**, 4045 (2003).

[26] E. Estevez-Rams, A. Penton-Madrigal, J. Martínez-García, and H. Fuess, Cryst. Res. Technol. **40**, 166 (2005).

[27] Inorganic Crystal Structure Database (ICSD), v. 1.4.4, (2008).

[28] W. A. Rachinger, J. Sci. Instrum. **25**, 254 (1948).

[29] R. Delhez, and E. J. Mittemeijer, J. Appl. Crystallogr. **8**, 609 (1975).

[30] Krumm SS. WINFIT 1.0 - A public domain program for interactive profile analysis under WINDOWS. XIIIth Conf. Clay Mineralogy and Petrology, Prague 1994. Acta Univ. Carolinea Geol. **38**, 253, (1994).

[31] B.E. Warren, B.L. Averbach, J. Appl. Phys. **21**, 595 (1950).

[32] Mathematica, Wolfram Research v. 11.2.